

Marker-free Registration for Electromagnetic Navigation Bronchoscopy under Respiratory Motion

Marco Feuerstein^{1,2}, Takamasa Sugiura², Daisuke Deguchi², Tobias Reichl^{1,2},
Takayuki Kitasaka³, Kensaku Mori^{2,4}

¹ Computer Aided Medical Procedures (CAMP), Technische Universität München,

² Graduate School of Information Science, Nagoya University,

³ Faculty of Information Science, Aichi Institute of Technology,

⁴ Information and Communications Headquarters, Nagoya University.

Abstract. Electromagnetic navigation bronchoscopy requires the accurate registration of a preinterventional computed tomography (CT) image to the coordinate system of the electromagnetic tracking system. Current state-of-the-art registration methods are manual or do not explicitly take patient's respiratory motion and exact airway shape into account, leading to relatively low accuracy. This paper presents an automated registration method addressing these issues. Electromagnetic tracking data recorded during bronchoscopic examination is matched to the airways by an optimizer utilizing the Euclidean distance map to the centerline of the airways for automated registration. Using a cutaneous sensor on the chest of the patient allows us to approximate respiratory motion by a linear deformation model and adopt the registration result in real time to the current respiratory phase. A thorough *in silico* evaluation on real patient data including CT images taken in 10 respiratory phases shows the significant registration error decrease of our method compared to the current state of the art, reducing the error from 3.5 mm to 2.8 mm.

1 Introduction

Bronchoscopy is a useful tool in the diagnosis and treatment of lung and bronchus cancer, for example to perform transbronchial biopsies of suspicious lymph nodes or pulmonary nodules. However, due to the complexity of the airways and the limited view during bronchoscopy, it is still difficult for a bronchoscopist to advance the bronchoscope and the biopsy needle to a peripheral target without the aid of fluoroscopy. To overcome this limitation, navigation systems have been proposed that localize and visualize the bronchoscope camera and biopsy needle in relation to a preinterventional computed tomography (CT) image and predefined targets and paths within the image [1, 2]. Accurate navigation is essential to guide camera and needle to small targets of only a few millimeters or centimeters.

Such a navigation system requires continuous tracking of the bronchoscope, for which various techniques have been proposed. Image based techniques try to register virtual camera images generated from preinterventional computed tomography data to the real images acquired by the bronchoscope camera [3, 4], which can be time-consuming and fail to continuously track the camera motion. Continuous and real-time electromagnetic tracking (EMT) of a small sensor coil attached to the bronchoscope tip can resolve these issues. Promising initial clinical results have been achieved using such an electromagnetic navigation bronchoscopy system [1].

Electromagnetic navigation bronchoscopy requires the registration between the coordinate system of the preinterventional CT image and that of EMT. In a commercially available system, this is performed by identifying about 5 to 9 landmarks in CT image coordinates by mouse clicks and in EMT coordinates by measuring their corresponding points with the sensor [1]. This is an unnatural and time-consuming process of several minutes and does not consider deformations of the airways caused by patient motion, mainly due to respiratory motion.

To deal with patient motion, Gergel et al. propose to apply particle filtering to each camera position acquired via EMT and project it to a previously segmented centerline of the airways [5], while Soper et al. combine electromagnetic tracking, image based tracking, Kalman-filtering, and a respiratory motion compensation method utilizing a surrogate sensor [6]. However, these techniques still require a manual marker-based registration between the CT and the EMT coordinate system. Automated registration methods were therefore proposed, which collect EMT data during bronchoscope movement inside the airways and match this data with airways previously extracted in CT images to obtain a global rigid transformation [7, 8]. Even if virtual breathing motion is added for evaluation in a static phantom [9], the resulting transformation matrix does not incorporate dynamic deformations caused by e.g. patient breathing, making the registration inaccurate. Furthermore, some methods [7, 9] assume all branches of the airway tree utilized during matching to be straight, which is rarely true for most airways.

In this paper we address the issues of previously proposed automated registration approaches [7–9]. We present a marker-free method that incorporates respiratory motion information and a better representation of the airway shape into the registration process. This significantly increases registration and navigation accuracy, as shown in our *in silico* evaluation.

2 Method

A part of our method follows previous works [7–9]. First the major airway branches, their centerline, and their tree structure are automatically extracted from a preinterventional CT image of the patient. Before bronchoscopy, an EMT sensor is inserted into the working channel of the bronchoscope and advanced to its tip or, alternatively, fully integrated into the bronchoscope tip not to obstruct the working channel. During bronchoscopic examination of the major airway branches, EMT data of this sensor is recorded and matched to the ex-

tracted airways. Compared to previous works, our new method presented here refines the matching strategy and takes respiratory motion into account, which significantly improves registration and navigation accuracy.

2.1 Respiratory Phase Detection

To acquire surrogate data for the estimation of respiratory motion we use a second cutaneous EMT sensor attached to the patient’s chest [6, 10], so for each bronchoscope sensor measurement we can obtain a corresponding cutaneous sensor measurement. The main purpose of this cutaneous sensor is to estimate a linear mapping between its motion and the patient’s respiratory motion.

When our matching procedure is started, a principal component analysis is performed on all cutaneous sensor positions obtained to date to compute their principal motion axis. All cutaneous sensor positions are then projected onto this axis and scaled to lie between 0 and 1, giving our surrogate data. Its local minima and maxima approximately correspond to full patient inspiration and expiration or vice versa. As we can be fairly safe to say that also the CT image was taken in either inspiration or expiration breath hold, as this is the standard procedure for chest CT, we now only need to determine, whether the minima of the ground truth data correspond to inspiration or expiration, which is done automatically in the next step.

2.2 Rigid Registration

During rigid registration, we compute the Euclidean transformation ${}^{\text{CT}}\mathbf{T}_{\text{EMT}}$ from EMT coordinates to CT coordinates using the bronchoscope sensor poses closest to the approximate respiratory phase the CT was acquired in. As CT data sets used for navigation can come from various hospitals and scanners sometimes without any information about whether their respiratory phase was inspiration or expiration, to estimate the correct phase we simply perform two rigid registrations, one only including bronchoscope sensor poses corresponding to surrogate sensor data between 0 and 0.1 and the other one only including bronchoscope sensor poses corresponding to surrogate data between 0.9 and 1. We then simply select the resulting transformation, which better corresponds to the CT data.

Each rigid registration is executed following the method proposed in [9], which can be seen as an iterative closest point-like approach, where all EMT points gradually converge to the airway tree. However, we can greatly improve registration performance by changing the error term used in [9] during optimization of the transformation matrix. Instead of finding the closest point on the straight line segments of the tree representation of the airways to a bronchoscope sensor position (transformed into CT coordinates) and computing their distance, we minimize the distance to the curved airway centerline. This can be achieved effectively by generating a Euclidean distance map d to the centerline obtained during airway segmentation, which is squared and normalized by division of each voxel by the average radius of the branch closest to the voxel. This

gives less weight to thick branches than to thin ones, and corresponds to the fact that bronchoscope movement naturally deviates much more from the centerline in thick branches than in thin branches.

In detail, our new error term is

$$Err(\mathbf{T}_{EMT}^{CT}) = \sum_{\mathbf{p}_k \in \mathcal{P}, s_{\min} \leq s(\mathbf{p}_k) \leq s_{\max}} \frac{1}{r_k} \cdot d^2(\mathbf{T}_{EMT}^{CT} \mathbf{p}_k), \quad (1)$$

where \mathbf{p}_k is the k th of N bronchoscope sensor positions, \mathbf{T}_{EMT}^{CT} transforms \mathbf{p}_k from EMT to CT coordinates, $s(\mathbf{p}_k)$ gives the surrogate data (between 0 and 1) corresponding to \mathbf{p}_k , s_{\min} and s_{\max} are set once to 0 and 0.1 and once to 0.9 and 1, respectively, r_k is the average radius of the branch closest to \mathbf{p}_k , and $d(\mathbf{x})$ returns the distance of our Euclidean distance map for a point \mathbf{x} . To determine the six degrees of freedom of \mathbf{T}_{EMT}^{CT} , the error is minimized using the CONDOR algorithm [11].

After performing the optimization twice, we divide each resulting error by the number of sensor positions. The lower normalized error will naturally correspond to the sensor data acquired in the respiratory phase close to the phase the CT was acquired in. Accordingly, in the following we choose the resulting transformation \mathbf{T}_{EMT}^{CT} with lower error and set the respiratory phase p_{CT} of CT acquisition to either 0 (approximately corresponding to the result using surrogate data between 0 and 0.1) or 1 (for surrogate data between 0.9 and 1).

2.3 Respiratory Motion Correction

After determination of the best respiratory phase and rigid matching between CT and EMT coordinates, we now apply an additional translation \mathbf{t}_{cor} that is scaled linearly with the respiratory phase measured by the surrogate sensor to correct for breathing motion. Even though this is just a rough approximation of the real deformation that is in fact a spatially varying deformation field, we will see later in our experiments that our simple linear scaling approach can already estimate the main bronchial motion well, as also shown in [6]. It can greatly improve registration accuracy without knowing a dense patient-specific deformation field that is rarely available for navigated bronchoscopy because of its necessity for several CT images of two or more respiratory phases.

In this second optimization step we again utilize CONDOR [11] to find a translation \mathbf{t}_{cor} that minimizes the error

$$Err(\mathbf{t}_{cor}) = \sum_{\mathbf{p}_k \in \mathcal{P}} \frac{1}{r_k} \cdot d^2 \left(\underbrace{\begin{pmatrix} \mathbf{I} & \|p_{CT} - s(\mathbf{p}_k)\| \mathbf{t}_{cor} \\ \mathbf{0}^T & 1 \end{pmatrix}}_{=: \mathbf{p}_{k_{cor}}} \mathbf{T}_{EMT}^{CT} \mathbf{p}_k \right). \quad (2)$$

3 Evaluation

Our institution does not yet permit us to evaluate our experimental electromagnetic navigation bronchoscopy system *in vivo*. Moreover, it is not a trivial task

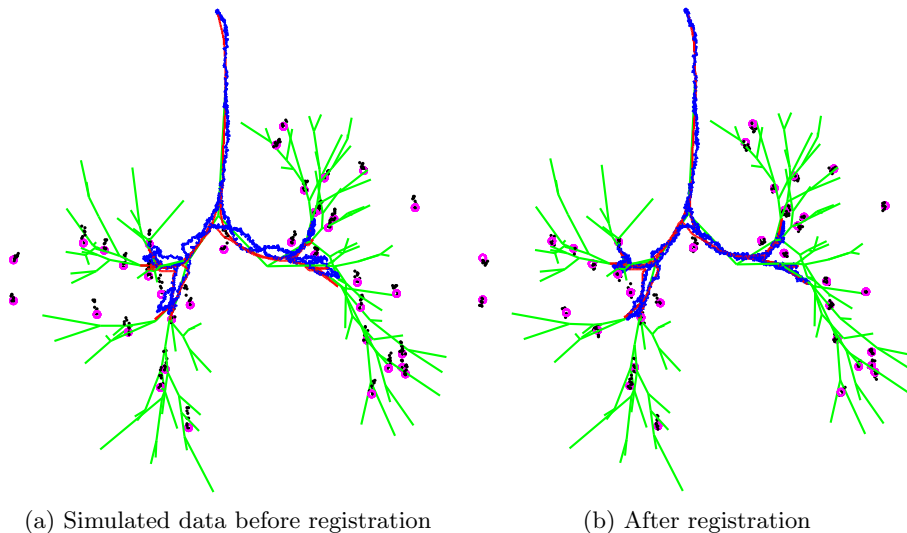


Fig. 1: Results of our *in silico* evaluation, showing airway tree line segments in green, a ground truth bronchoscope path in red, a simulated path (before and after registration) in blue, ground truth landmarks in pink, and their deformed counterparts (before and after registration) in 10 breathing phases in black.

to generate ground-truth data and perform a quantitative evaluation of electromagnetic navigation bronchoscopy in the operating room without significantly changing the current clinical work flow. This may be solved by deformable physical phantoms, but they are still far from realistic respiratory motion modeling, and for those the quantification of ground truth motion is still an open question, too. We hence decided to set up a thorough *in silico* evaluation on real patient CT data with exhaustive and accurate breathing information. Therefore we use the POPI model [12], which contains 10 respiratory phases and provides dense deformation fields between all phases as well as landmarks chosen by medical experts and widely distributed inside the lungs and around the airways⁵.

We selected the end-inhalation phase of the POPI data to serve as the single CT image that is usually acquired before bronchoscopy. In this CT image we extracted the airways, their centerline, and their tree structure (marked green in Fig. 1a) using our previously proposed method [13], and simulated 10 different bronchoscope paths and their corresponding bronchoscope EMT sensor data. Each bronchoscope path was created using a few manually selected keyframes in every branch close to, but not on its centerline and connecting the frames by Catmull-Rom splines and Slerp quaternion interpolation. It can be adjusted to cover a certain number of airway generations, e.g. 1 referring to the trachea, 2 to the trachea and left and right main bronchi, 3 to the trachea, left and right

⁵The data was obtained from the Léon Bérard Cancer Center & CREATIS lab, Lyon, France; <http://www.creatis.insa-lyon.fr/rio/popii-model>

main bronchi, left and right upper lobe bronchi, left lower lobe bronchus and right truncus intermedius, and so on. We set the speed of the bronchoscope to 10 mm/s, as this is a good approximation of the average speed during bronchoscopy [4]. The sampling rate was set to 40 Hz, according to the frequencies of typical EMT systems such as the NDI Aurora or the Ascension 3D Guidance medSAFE. These data serve as our ground truth bronchoscope paths (marked red in Fig. 1a).

However, as EMT has a significant amount of distortion and jitter, we also added normally distributed noise to the ground truth tracking data to create a more realistic simulation of the bronchoscope paths. According to [14], we set the standard deviation of the noise for a bronchoscope sensor position to 1 and hence for each of its three translational components to $1/\sqrt{3}$. According to the specifications for the orientation accuracy of the NDI tracker⁶ and its corresponding orientation distortion for a metal sheet similar to an operating table [15], we set the noise for each of the three Euler angles of a measured camera pose to $\sqrt{(\frac{1}{2} \cdot 0.5)^2 + (\frac{1}{2} \cdot 1.2)^2}/\sqrt{3} = 0.65/\sqrt{3}$.

Once noise is added to the bronchoscope path, assuming normal breathing frequency of 12 breaths per minute, we can transform each sample along the path according to its respiratory information. For this we apply linear interpolation between the 10 respiratory phases to care for inter-phase motion as well as within each deformation field to care for inter-voxel spaces (a resulting bronchoscope path including noise and respiratory motion is marked blue in Fig. 1a). At the same time, to simulate cutaneous sensor measurements for our surrogate data, we select a point at the patient’s chest wall and apply the same sampling rate and respiratory motion as for the bronchoscope sensor. However, since the cutaneous sensor only moves within a very limited volume up to about 10 mm and is hence only marginally affected by distortion and systematic error, we only need to take measurement precision into account when simulating error, so according to the specifications of NDI⁶ we set its standard deviation for x -, y -, and z -direction (i.e. along the left-right, superior-inferior, and anteroposterior axes) to $(\frac{1}{2} \cdot 0.9)/\sqrt{3} = 0.45/\sqrt{3}$.

Finally, we apply a Euclidean transformation to all simulated sensor measurements, so they lie outside the coordinates of the original CT volume. As now ground truth and simulated data do not overlap any more, we rule out this trivial solution for the optimizer.

For evaluation of the final registration accuracy, we used 37 of the 41 widely distributed landmarks in the POPI model provided by medical experts as ground truth, which are inside the lungs or close to the airways (three of the POPI landmarks are outside these regions, one is an image artifact). These landmarks serve as target points for e.g. biopsies and are not in close proximity to the simulated bronchoscope path used for registration. In our simulation environment, we apply the same noise to these landmarks as to the bronchoscope sensor, deform them according to 10 respiratory phases, and transform them to be outside the original CT volume in the same way as for the bronchoscope path. Figure 1a

⁶<http://www.ndigital.com/medical/aurora-techspecs-performance.php>

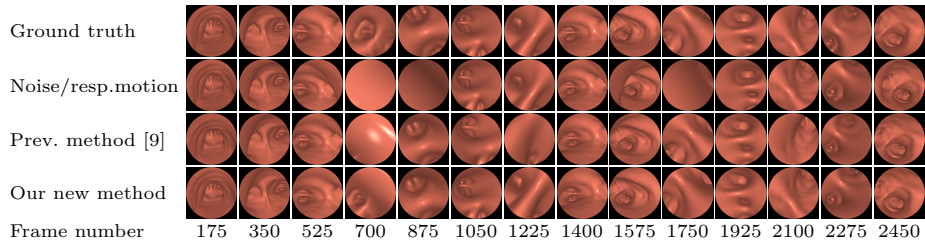


Fig. 2: Exemplary frames of a bronchoscope path, showing ground truth data (first row), after adding noise and respiratory motion (second row), and corresponding renderings after registration with a previous method [9] (third row) and our new method (fourth row).

shows the ground truth landmarks in pink and their corresponding ones in 10 different respiratory phases including noise in black. After obtaining ${}^{\text{CT}}\mathbf{T}_{\text{EMT}}$ and \mathbf{t}_{cor} by our two-step registration approach, we can now transform each simulated landmark \mathbf{p}_l to $\mathbf{p}_{l_{\text{cor}}}$ according to Eq. 2 and compare it to the ground truth data.

Figure 1b shows a bronchoscope path and evaluation landmark positions after applying our registration and motion compensation method. Figure 2 shows exemplary frames of a bronchoscope path (using four branch generations) for ground truth data and after adding noise and respiratory motion as well as the resulting paths after registration with a previously proposed method [9] and our new method. The supplementary video demonstration⁷ shows all frames of this path and allows the observer to qualitatively evaluate the performance of our registration method. Table 1 quantitatively compares the registration error of our new method to [9]. We also integrated only the new error term of Eq. 1 into [9] to outline individual accuracy differences.

The runtime of our registration method on a PC with an Intel Xeon X5355 processor was between 1 and 3 seconds and mainly depends on the number of branch generations and hence sample points created along the bronchoscope path.

4 Discussion

As can be seen in Table 1, all methods perform better the more airway generations are covered during registration, so we suggest to perform a registration after exploring as many branches as possible. A one-way analysis of variance (ANOVA) over the 3700 samples (10 paths, 10 respiratory phases, and 37 landmarks) of each case confirms that our new registration method significantly

⁷http://campar.in.tum.de/files/publications/feuerste2010miar.video_path_without_noise.avi and http://campar.in.tum.de/files/publications/feuerste2010miar.video_path_with_noise.avi

Table 1: Registration error in mm over all 10 simulated bronchoscope paths according to absence or presence of noise, number of airway generations and bronchoscope path samples, respiratory phase used to compute the landmark registration error, error term, and utilization of respiratory motion correction.

Noise	Gen.	Samples	Phase	Registration error [mm]					
				No respiratory motion correction [9]			New method (Resp. mot. corr. & new error term)		
				Old error term [9]			New error term		
w/o	2	1319 ±22	1 2 3 4 5	5.3 4.9 4.6 5.0 5.5	4.6 4.2 3.9 4.5 5.4	4.2 4.3 4.1 4.2 4.5			
			10 9 8 7 6	5.2 4.7 4.7 5.2 5.6	4.4 4.1 4.4 5.1 5.7	4.2 4.3 4.5 4.5 4.7			
			avg	5.1 ± 2.3	4.6 ± 2.3	4.3 ± 2.4			
	3	1815 ±24	1 2 3 4 5	5.0 4.5 4.2 4.6 5.1	3.2 2.6 2.2 3.0 4.1	1.4 1.7 2.4 2.9 3.3			
			10 9 8 7 6	4.7 4.2 4.1 4.7 5.2	2.9 2.4 2.7 3.7 4.4	1.8 2.1 2.7 3.1 3.5			
			avg	4.6 ± 2.1	3.1 ± 1.7	2.5 ± 1.4			
	4	2754 ±25	1 2 3 4 5	3.9 3.3 2.6 3.1 4.0	3.0 2.5 2.0 2.9 4.0	2.0 2.2 2.3 2.5 2.8			
			10 9 8 7 6	3.5 2.9 2.8 3.3 4.2	2.5 1.8 2.1 3.3 4.2	2.0 2.2 2.4 2.5 3.0			
			avg	3.4 ± 1.8	2.8 ± 1.5	2.4 ± 1.4			
w	2	1319 ±22	1 2 3 4 5	5.4 4.8 4.6 4.9 5.6	4.6 4.0 4.0 4.4 5.5	4.6 4.5 4.5 4.5 4.9			
			10 9 8 7 6	5.2 4.7 4.6 5.4 5.6	4.4 4.2 4.5 5.4 5.8	4.5 4.7 4.8 5.0 5.1			
			avg	5.1 ± 2.4	4.7 ± 2.3	4.7 ± 2.5			
	3	1815 ±24	1 2 3 4 5	5.0 4.3 4.2 4.6 5.1	3.4 2.6 2.4 3.0 4.2	3.2 3.2 3.9 4.1 4.6			
			10 9 8 7 6	4.8 4.1 3.9 4.9 5.2	3.0 2.6 2.8 3.9 4.5	3.5 3.7 4.0 4.5 4.8			
			avg	4.6 ± 2.1	3.2 ± 1.7	4.0 ± 3.7			
	4	2754 ±25	1 2 3 4 5	4.1 3.4 2.9 3.0 4.1	3.1 2.5 2.3 2.9 4.1	2.4 2.4 2.8 2.7 3.3			
			10 9 8 7 6	3.7 3.1 3.0 3.5 4.2	2.7 2.1 2.4 3.5 4.4	2.5 2.6 2.8 3.0 3.4			
			avg	3.5 ± 1.8	3.0 ± 1.5	2.8 ± 1.6			

outperforms the previous method [9] with a p -value of 0.000 in all cases. This is because it successfully utilizes the actual curved shape of the airways in contrast to [9] only using straight line segments. Furthermore, our new method first tries to find the bronchoscope sensor phase best matching the CT data and based on that linearly adjusts the respiratory motion offset. The positive effect of this adjustment can be seen e.g. in frames 700, 1225, and 2100 of Fig. 2.

In the presence of noise, our method showed some outliers when registration was performed using 3 airway generations, leading to an error of 4.0 ± 3.7 mm. As we attribute this behavior to too noisy cutaneous sensor data, we repeated our experiments only adding noise to the bronchoscope sensor, but not to the cutaneous sensor, simulating a perfect respiratory signal. Since this reduced the registration error for 3 airway generations from 4.0 ± 3.7 mm and for 4 generations from 2.8 ± 1.6 mm to 2.6 ± 1.3 mm, we are now considering using a more reliable technique for measuring respiratory motion such as an elastic belt placed around the abdomen, which is a well established means for gated 4D CT and MR, SPECT, and PET-CT imaging as well as radiation therapy, or, if a belt is not available, a method to denoise the surrogate data and match it to a realistic respiratory curve.

While for the previous method error is distributed over all 10 breathing phases, for our method it is significantly lower, but at the same time increases between end-inhalation (phase 1) and end-exhalation (phase 6). This confirms that our registration method approximates patient breathing well, but still not to its full extent. One may hence think of matching a (readily available) dense deformation field of another patient to the current patient to obtain a more accurate

estimation of dense respiratory displacements instead of using a linearly scaled translational offset for breathing compensation. However, our current results using a simple and fast approach for automated registration are very promising. As soon as permission is granted by our institution, we will also evaluate our method *in vivo*.

In our experiments we also tested other methods to compensate for respiratory motion such as scaling the tracking data (as lung motion is bigger at the diaphragm than towards the superior) and rotating all branches around their branching points (as their motion is not completely linear). However, a simple translation gave the best results. When optimizing translation and scaling at the same time, the registration error for the case of four airway generations and noisy data increased to 2.9 to 3.9 mm (compared to 2.8 mm), depending on the choice of which axes to scale and the position of the scaling center along the craniocaudal axis. We attribute this to an overfitting of the tracking data to the bronchial tree due to additional degrees of freedom. When optimizing scaling only, the registration error was 4.0 to 4.3 mm.

The automatic approach for phase determination using only rigid registrations at first glance may sound paradoxical under the assumption of a linear respiratory motion model. However, it works well, because the translation assumed for respiratory motion compensation is only an approximation of the real deformation, which is more complex. Under this complex deformation it should be clear that a CT rigidly registered to tracking data from the same phase should fit better than to tracking data from a different deformed phase. Our initial rigid registration only considers two subsets of the tracking data, and only yields a single transformation. The second registration then includes all tracking data and yields an additional time-dependent translation which approximates the respiratory motion.

Finally, our method currently only addresses respiratory motion. We are planning to also add methods for the handling of other kinds of patient motion, for instance one that is able to exclude outliers from surrogate data caused by e.g. coughing.

5 Conclusion

This paper successfully reduces registration error caused by respiratory motion and insufficient utilization of the correct airway shape during optimization. Using the POPI model, we are able to provide a very realistic respiratory motion simulation with real patient data, making a laborious *in vivo* experiment unnecessary for a first thorough evaluation. Our evaluation shows that our new automated marker-free registration method is significantly more accurate than the current state of the art [9]. Even for noisy data, as it is the case for EMT data, our method performs robust and reduces the registration error from 3.5 mm to 2.8 mm.

References

1. Eberhardt, R., Anantham, D., Herth, F., Feller-Kopman, D., Ernst, A.: Electromagnetic navigation diagnostic bronchoscopy in peripheral lung lesions. *Chest* **131**(6) (2007) 1800–1805
2. Bertoletti, L., Robert, A., Cottier, M., Chambonniere, M.L., Vergnon, J.M.: Accuracy and feasibility of electromagnetic navigated bronchoscopy under nitrous oxide sedation for pulmonary peripheral opacities: An outpatient study. *Respiration* **78**(3) (2009) 293–300
3. Bricault, I., Ferretti, G., Cinquin, P.: Registration of real and CT-derived virtual bronchoscopic images to assist transbronchial biopsy. *IEEE Trans. Med. Imag.* **17**(5) (1998) 703–714
4. Rai, L., Helferty, J.P., Higgins, W.E.: Combined video tracking and image-video registration for continuous bronchoscopic guidance. *Int J CARS* **3** (2008) 315–329
5. Gergel, I., dos Santos, T.R., Tetzlaff, R., Maier-Hein, L., Meinzer, H.P., Wegner, I.: Particle filtering for respiratory motion compensation during navigated bronchoscopy. In: *SPIE Medical Imaging*. (2010)
6. Soper, T.D., Haynor, D.R., Glenny, R.W., Seibel, E.J.: In vivo validation of a hybrid tracking system for navigation of an ultrathin bronchoscope within peripheral airways. *IEEE Trans. Biomed. Eng.* **57**(3) (2010) 736–745
7. Deguchi, D., Ishitani, K., Kitasaka, T., Mori, K., Suenaga, Y., Takabatake, H., Mori, M., Natori, H.: A method for bronchoscope tracking using position sensor without fiducial markers. In: *SPIE Medical Imaging*. (2007)
8. Klein, T., Traub, J., Hautmann, H., Ahmadian, A., Navab, N.: Fiducial-free registration procedure for navigated bronchoscopy. In: *MICCAI*. (2007)
9. Mori, K., Deguchi, D., Kitasaka, T., Suenaga, Y., Hasegawa, Y., Imaizumi, K., Takabatake, H.: Improvement of accuracy of marker-free bronchoscope tracking using electromagnetic tracker based on bronchial branch information. In: *MICCAI*. (2008)
10. Borgert, J., Krüger, S., Timinger, H., Krücker, J., Glossop, N., Durrani, A., Viswanathan, A., Wood, B.J.: Respiratory motion compensation with tracked internal and external sensors during CT-guided procedures. *Comput. Aided Surg.* **11**(3) (2006) 119–125
11. Vanden Berghen, F., Bersini, H.: CONDOR, a new parallel, constrained extension of powell’s UOBYQA algorithm: Experimental results and comparison with the DFO algorithm. *J. Comput. Appl. Math.* **181** (2005) 157–175
12. Vandemeulebroucke, J., Sarrut, D., Clarysse, P.: The POPI-model, a point-validated pixel-based breathing thorax model. In: *ICCR*. (2007)
13. Feuerstein, M., Kitasaka, T., Mori, K.: Automated anatomical likelihood driven extraction and branching detection of aortic arch in 3-D chest CT. In: *Second International Workshop on Pulmonary Image Analysis*. (2009) 49–60
14. Wegner, I., Tetzlaff, R., Biederer, J., Wolf, I., Meinzer, H.P.: An evaluation environment for respiratory motion compensation in navigated bronchoscopy. In: *SPIE Medical Imaging*. (2008)
15. Kirsch, S.R., Schilling, C., Brunner, G.: Assessment of metallic distortions of an electromagnetic tracking system. In: *SPIE Medical Imaging*. (2006)